

MEC Task Offloading in AIoT: A User-Centric DRL Model Splitting Inference Scheme

LI Weixi¹, GUO Rongzuo^{1*}, WANG Yuning², CHEN Fangying¹

1. College of Computer Science, Sichuan Normal University, Chengdu 610101, China;
2. Academic Affairs Office, Sichuan Water Conservancy Vocational College, Chongzhou 611231, China.

Abstract: With the rapid development of the Artificial Intelligence of Things (AIoT), mobile edge computing (MEC) becomes an essential technology underpinning AIoT applications. However, multi-angle resource constraints, multi-user task competition, and the complexity of task offloading decisions in dynamic MEC environments present new technical challenges. Therefore, a user-centric deep reinforcement learning (DRL) model splitting inference scheme is proposed to address the problem. This scheme combines model splitting inference technology and designs a UCMS_MADDPG-based offloading algorithm to realize efficient model splitting inference responses in the dynamic MEC environment with multi-angle resource constraints. Specifically, we formulate a joint optimization problem that integrates resource allocation, server selection, and task offloading, aiming to minimize the weighted sum of task execution delay and energy consumption. We also introduce a user-server co-selection algorithm to address the selection issue between users and servers. Furthermore, we design an algorithm centered on user pre-decision to coordinate the outputs of continuous and discrete hybrid decisions, and introduce a priority sampling mechanism based on reward-error trade-off to optimize the experience replay mechanism of the network. Simulation results show that the proposed UCMS_MADDPG-based offloading algorithm demonstrates superior overall performance compared with

other benchmark algorithms in dynamic environments.

Keywords: Artificial intelligence of things, mobile edge computing, deep reinforcement learning, task offloading

This work was supported by Natural Science Foundation of China (11905153). Weixi Li, female, master, research direction is mobile edge computing, E-Mail: liweixi@stu.sicnu.edu.cn; Rongzuo Guo, male, master, professor, master's supervisor, research directions include embedded systems, IoT perception technology, system reliability, and intelligent control, E-Mail: gyz00001@163.com.

1 Introduction

The convergence of artificial intelligence (AI) and Internet of Things (IoT) has resulted in the Artificial Intelligence of Things (AIoT) [1], which shows broad application prospects in many fields. By combining the automated analysis and decision-making capabilities of AI with the extensive connectivity and real-time data collection capabilities of IoT, AIoT effectively enhances system intelligence and promotes the digital and intelligent transformation of traditional industries. However, AIoT also faces technical challenges in practical applications, primarily due to the large volume and heterogeneity of data generated by IoT devices, which impose significant demands on system computing architectures. Traditional cloud computing (CC) [2] relies on centralized data centers to process, store, and analyze data, and has previously demonstrated good adaptability to IoT applications. Nevertheless, as the number of IoT devices has surged and application scenarios have diversified, traditional cloud computing architectures increasingly struggle to meet the stringent requirements of AIoT in terms of real-time responsiveness, efficiency, and low-carbon sustainability. This limitation results from high transmission latency, inefficient bandwidth utilization, and substantial energy consumption associated with centralized processing. To address these issues, mobile edge computing (MEC)[3] emerges as a promising solution. By offloading computing, storage, and networking functions to the network edge closer to end devices, MEC enables a computing paradigm characterized by low latency, improved bandwidth utilization, and enhanced energy efficiency. Despite its advantages in improving the computational efficiency of AIoT systems, MEC still faces challenges such as limited computing capacity and constrained resources. Therefore, how to

intelligently manage resources and optimize task offloading strategies remains a critical research problem in MEC.

The task offloading of MEC in AIoT is commonly addressed using deep reinforcement learning (DRL), where the computational task offloading process is formulated as a Markov decision process (MDP), enabling the optimization of offloading decisions within the MEC system[4-7]. For instance, Wu et al. [8] proposed a hybrid offloading strategy that integrated convex optimization with a deep Q-network (DQN) to optimize task offloading in time-varying fading channels, and demonstrated good performance in large-scale networks. Hu et al. [9] addressed the task offloading problem under time-varying channels by formulating it as the minimization of the average long-term service cost, considering both power consumption and buffer delay in dynamic task patterns. To tackle the mixed action space involving continuous and discrete decisions, they employed a combination of deep deterministic policy gradient (DDPG) and dueling double deep Q-network (D3QN). Compared with DQN, the proposed algorithm achieved significant performance improvement. Due to limitations in computing power and resources on user devices and MEC servers, task offloading decision algorithms are required to handle discrete, continuous, and hybrid action spaces. However, both DQN and DDPG exhibit limitations when applied to large discrete action spaces [10] or hybrid action spaces that combine continuous and discrete decisions [11], restricting their practicality in complex real-world environments. Although task offloading algorithms based on multi-agent deep deterministic policy gradient (MADDPG) are well-suited for continuous action spaces, effectively representing and jointly optimizing both discrete and continuous action spaces remains a significant challenge [12].

Numerous existing studies have considered the constraints imposed by limited wireless communication resources and server-side computational capacity, including the restricted local computing power and finite battery energy of user devices [13,14], and computing resource limitation on the MEC server [15]. To address these challenges, various solutions have been proposed, such as leveraging cloud-edge collaboration (MEC-MCC) [15] or enabling cooperative computation among multiple MEC servers [16]. However, in the existing DRL-based task offloading algorithms [18-24], the limitation of server storage resources has received less attention. To better align with real-world environments, we consider the multi-angle resource constraints of user devices and MEC servers, and adopt a user-centric model splitting inference technology

to enable task offloading decision-making and response. Model splitting inference [25] is a technique that optimizes the inference performance of deep learning models in resource-constrained environments. The core idea is to divide a complex deep neural network (DNN) model into several parts (or sub-models), perform the first half of the inference on the end device, transmit the intermediate result to the edge server, and complete the second half of the inference on the edge side. With a suitable splitting strategy, this approach can significantly reduce inference delay and end-side energy consumption, at the cost of a certain communication overhead [26].

The key contributions of this paper include:

- We propose a dynamic MEC environment with multiple users and servers in AIoT, focusing on the task processing problem of end users in service areas where multiple servers overlap. The model considers multi-angle resource constraints, including communication resources, user device resources, user computing capacity, and server storage capacity.
- To simplify the optimization problem, we decouple it into a user-server selection problem and a task offloading problem. We design a user-server co-selection algorithm to address the selection and matching between users and servers.
- A hybrid decision support UCMS_MADDPG algorithm, using a user-centric model splitting inference scheme. With user decisions as the primary driver, servers contribute to offloading decisions. The pre-decision for resource allocation and task offloading is first made on the user-side CPU and then refined on the server-side CPU to complete the hybrid decision process.
- We perform comprehensive experiments, including ablation analysis and comparisons with various heuristic baselines, to verify the proposed algorithm's performance.

The structure of this paper is as follows. Section 2 reviews the related work. In Section 3, we present the system model and formulate the optimization problem. Section 4 analyzes the problem and proposes corresponding solutions. Section 5 discusses the simulation results. Finally, Section 6 concludes the paper.

2 Related Work

Many scholars have conducted extensive research on MEC task offloading strategy optimization. Among these approaches, the use of DRL techniques to address task offloading and resource allocation in MEC environments has become their main concern. Huang et al. [4] investigated low-complexity task offloading strategies and proposed a linear programming relaxation (LR)-based algorithm, along with a distributed deep learning-based offloading (DDLO) approach, to ensure service quality in MEC networks while minimizing the energy consumption of user devices. Li et al. [5] focused on joint computation and communication optimization for user devices handling multiple tasks in UAV-assisted MEC networks, introducing a multi-agent proximal policy optimization (MAPPO) framework with beta distribution to jointly optimize UAV trajectories, task partitioning, and the overall weighted energy consumption. Yan et al. [6] applied a long short-term memory (LSTM) network enhanced with an attention mechanism, combined with the DDPG algorithm, to effectively reduce system latency in vehicular MEC networks. Mi et al. [7] developed a multi-agent online control (MAOC) algorithm based on MAPPO to handle delay-sensitive tasks in D2D-assisted MEC systems, which adjusted the CPU frequency of discrete time slots to make intelligent decisions, so as to reduce the load of edge servers and effectively prevent network congestion. The above research demonstrates the effectiveness of DRL in resource allocation and offloading optimization. However, these studies overlook the dynamic variations in user tasks and server resources in real-world environments. Instead, they conduct simulations based on fixed numerical values, lacking applicability to realistic dynamic scenarios.

In dynamic MEC environments, many scholars address the multi-objective joint optimization problem, focusing on communication and computing resource constraints to improve performance. This remains a complex challenge. Tariq et al. [15] proposed a DRL-driven energy-efficient task offloading (DEETO) scheme, which considers battery capacity and computing power limitations in UAV emergency scenarios. By implementing a hybrid task offloading mechanism, the energy consumption of UAV is minimized. Chen et al. [18] proposed a temporal attentional deterministic policy gradient (TADPG) method to jointly optimize resource allocation for multiple mobile devices in MEC systems, effectively reducing latency, energy consumption, and the

average long-term cost. Nguyen et al. [19] introduced a collaborative task offloading and block mining (TOBM) framework for blockchain-enabled MEC systems, which maximizes overall system utility. Gong et al. [20] examined dependent task adaptive offloading in dynamic networks, proposing a DRL-based dependent task offloading strategy (DTOS) that reduces latency and energy consumption in network services. Dong et al. [21] decomposed the problem into two parts. By using the TD3 algorithm to solve resource allocation (RA) under fixed task offloading decisions, By reusing heuristic particle swarm optimization (PSO) methods to solve task offloading guided by optimal value functions, their approach effectively reduces production time and energy consumption in industrial Zhang et al. [14] investigated highly dynamic MEC systems equipped with energy harvesting (EH) devices. They proposed a multi-device hybrid decision actor-critic algorithm to effectively manage the hybrid action space, encompassing both continuous and discrete decisions across devices, thereby balancing delay and energy consumption. IoT scenarios.

To address diverse resource constraints, several studies have explored MEC-MCC techniques or collaborative computation among multiple servers. Zhang et al. [14] investigated highly dynamic MEC systems equipped with energy harvesting (EH) devices, and proposed a multi-device hybrid decision actor-critic algorithm for dynamic task offloading. This algorithm effectively manages the hybrid action space, encompassing both continuous and discrete decisions across devices, thereby balancing delay and energy consumption. Wu et al. [16] developed an energy-efficient dynamic task offloading (EEDTO) algorithm for MEC-MCC environments supporting blockchain, optimizing the balance between computing power limitations, high latency, secure offloading, and data integrity. Yang et al. [17] introduced a global state-sharing model based on a variational recurrent neural network (VRNN) in distributed MEC systems, significantly reducing server communication overhead and task execution time. Zhao et al. [22] proposed a DRL algorithm with a hierarchical reward function for video offloading in MEC networks. This approach ensures video security, improves user quality of experience (QoE), and reduces energy consumption. Du et al. [23] addressed the challenge of real-time, efficient processing of intensive applications in healthcare IoT devices. They proposed a collaborative cloud-edge offloading model tailored for ultra-dense edge computing (UDEEC) networks, effectively reducing both energy consumption and task execution latency. Liu et al. [24] introduced a collaborative MEC framework that jointly optimizes resource allocation, offloading,

and service caching intending to maximize long-term QoS while reducing cache switching costs. In real-world environments, edge server resources are often limited. While the above studies consider the computational resource constraints of servers, they overlook storage resource limitations. Setting the storage resources of the server to an ideal state in a task-intensive state with a large number of users can effectively improve system utility, but also reduce its universality.

Table 1 summarizes a comparative analysis of representative existing works. As highlighted in the above review, DRL has proven effective in addressing complex joint optimization problems in MEC systems. However, in most of the research on dynamic environments, less consideration is given to the storage resource limitation of the server. Therefore, in the context of a dynamic AIoT environment with multiple users and multiple servers, we consider the multi-angle resource constraints of user devices and servers. The objective is to jointly optimize resource allocation, server selection, and task offloading strategies, aiming to minimize the weighted sum of task execution latency and energy consumption.

Table 1 Comparison of Existing Jobs

Paper	Objective	Method	Multiple servers	Dynamic environment	Energy limitation	Server computing resource limitation	Server storage resource limitation
Huang et al.[4]	Minimize energy consumption	LR-based and DDLO	✓	×	×	×	×
Li et al.[5]	Minimize energy consumption	b-MAPPO	✓	×	×	✓	×
Yan et al.[6]	Minimize latency	LDDPG	×	×	✓	×	×
Mi et al.[7]	Minimize latency	MAOC	×	×	✓	×	×
Tariq et al.[15]	Minimize energy consumption	DEETO	×	✓	✓	✓	×
Chen et al.[18]	Minimize latency and energy consumption	TADPG	×	✓	×	×	×
Nguyen et al.[19]	Maximizing system utility	MA-DRL	×	✓	×	×	×
Gong et al.[20]	Minimize latency and energy consumption	DTOS	×	✓	×	×	×
Dong et al.[21]	Minimize latency and energy consumption	TD3 and PSO	×	✓	×	×	×
Zhang et al.[14]	Minimize latency and energy consumption	MD Hybrid AC	✓	✓	✓	✓	×
Wu et al.[16]	Minimize latency and energy consumption	EEDTO and Lyapunov	✓	✓	×	×	×

Yang et al.[17]	Minimize latency	VRNN	✓	✓	×	✓	×
Zhao et al.[22]	Minimize energy consumption and maximize QoE	JVFRS-CO-RA-MADDPG	✓	✓	✓	✓	×
Du et al.[23]	Minimize latency and energy consumption	DDPG	✓	✓	×	×	×
Liu et al.[24]	Maximizing QoS and reducing costs	DGL-DDPG	✓	✓	✓	✓	×

3 System Model

The multi-edge server deployment in the MEC environment for AIoT is illustrated in Fig. 1. In this model, we assume that the servers do not have direct physical links for communication and independently process computing tasks within their respective service coverage areas. However, due to overlapping service regions between servers, an end user located in such a region can select to offload tasks to a specific server.

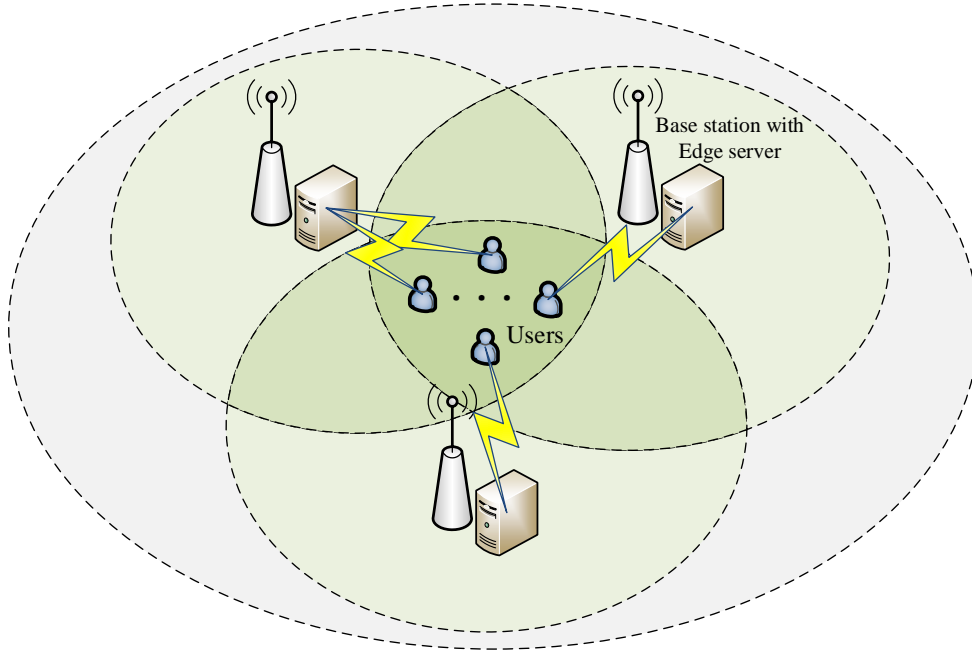


Fig.1 System environment layout

This section introduces the task model of the MEC system in the AIoT scenario, as shown in Fig. 2. We consider a set of M edge servers (ESs) with overlapping service areas and N user devices (UDs), each carrying out different tasks. The set of edge servers is denoted by $M = \{1, 2, \dots, m\}$, and the set of user devices is denoted by $N = \{1, 2, \dots, n\}$. Each ES is equipped with multiple CPUs and fixed storage capacity to provide both computing and storage services, while each UD is equipped with a single

CPU and battery. Task data is transferred between the ESs and UDs through the base station (BS) over a wireless transmission channel. The following section provides a detailed introduction to tasks, computing, and energy harvesting models.

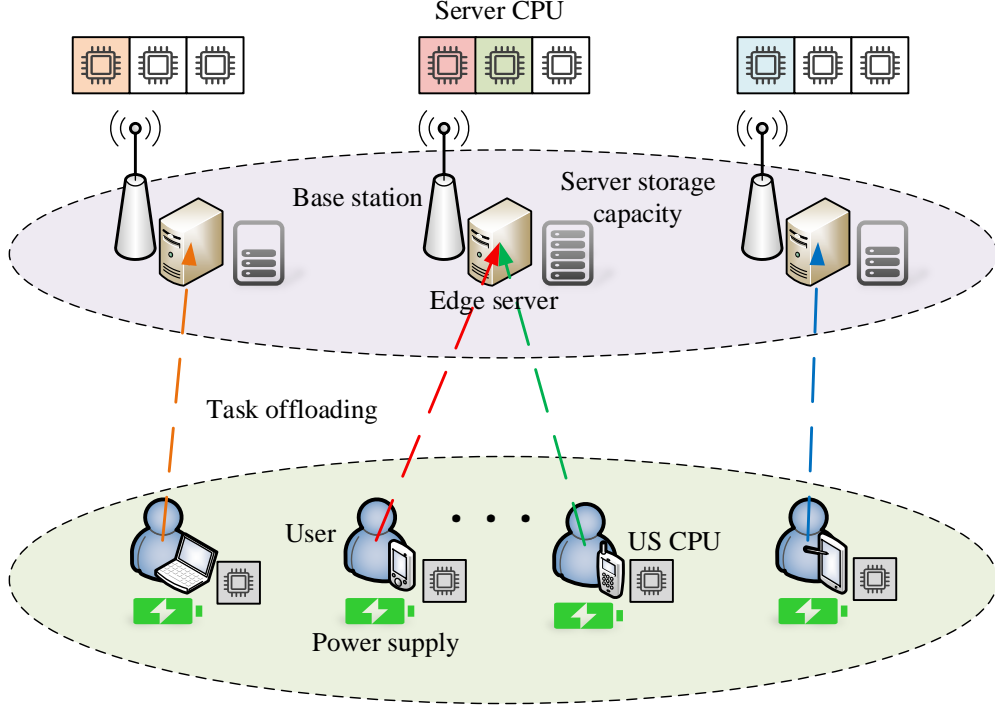


Fig.2 System task model

3.1 Task Model

Usually, the UD has limited computing power, and computing tasks are sensitive to delay. Therefore, we model task execution within discrete time slots, where $\varphi_{max}(t)$ denotes the maximum tolerated delay for task execution in each slot t , and the set of operational periods is denoted as $T = \{1, 2, \dots, t\}$. Each user device $UDn \in N$ is assumed to generate a random task at the beginning of each time slot $t \in T$, and if the task is not processed to completion within $\varphi_{max}(t)$, it will be discarded before the next time slot begins. The task generated by UDn in time slot t^1 is denoted by $(\beta_n(t), c_n(t), \varphi_n(t))$, where $\beta_n(t)$ represents the task size in bytes, and $c_n(t)$ denotes the number of CPU cycles required to process each bit of the task. The maximum allowable completion

¹ All the following formulas are evaluated within a single time slot t .

time for the task is given by $\varphi_n(t)$.

In an AIoT edge computing environment, the UD typically utilizes local computing, full offloading computing, and partial offloading computing to process tasks. In this paper, we focus on binary decision methods, specifically considering local computing and full offloading computing for handling UD tasks. The binary decision method $\mathbf{x} = \{x_n(t) | n \in N, t \in T\}$ is defined in Equation (1):

$$x_n(t) = \begin{cases} 1, & \text{MEC computing} \\ 0, & \text{Local computing} \end{cases} \quad (1)$$

if the UD n selects local computing, then $x_n(t) = 0$, and if the UD n selects offloading computing, $x_n(t) = 1$.

For a UD n in overlapping service regions, connections can be established with multiple ES, but only one ES can be selected by the UD for task offloading. Similarly, a binary decision is used to represent the UD selection, where $\mathbf{y} = \{y_{n,m}(t) | n \in N, m \in M, t \in T\}$ is defined in Equation (2):

$$y_{n,m}(t) = \begin{cases} 1, & \text{selection} \\ 0, & \text{otherwise} \end{cases} \quad (2)$$

if the UD n selects the ES $m \in M$ for computing during offloading, $y_{n,m}(t) = 1$, otherwise $y_{n,m}(t) = 0$.

Denote by $Z_m = \{z_m(t) | m \in M, t \in T\}$ the set of the UD n successfully connected to the ES m , where $z_m(t) = \sum_{n \in N} 1_{y_{n,m}(t)=1}$. To be more realistic, we stipulate that the UD that each ES can connect is limited, and define the maximum user capacity of the ES m as z_{max} , i.e., $z_m(t) \leq z_{max}$.

3.2 Local Computing Model

In the local computing model, each UD n is allocated a minimum and maximum local computing capacity, denoted as f_{min}^l and f_{max}^l (in GHz), respectively. This paper adopts a user-centric task offloading model where, if the UD n decides to compute the task locally, the ES m does not intervene. Furthermore, if the UD n requests task offloading to ES m , but ES m does not make a decision and opts to offload the task, the

task of UD will still be processed locally. Details are described in section 4.2.

Specifically, the local computing task delay $\tau_n^l(t)$ is determined according to the task size of the UD n and the allocation of computing capacity:

$$\tau_n^l(t) = \frac{\beta_n(t)c_n(t)}{f_n^l(t)} \quad (3)$$

where $f_n^l(t)$ is the computing power of UD n in time slot t , and the local computing power of UD n is limited to its allocation budget, i.e., $f_{min}^l \leq f_n^l(t) \leq f_{max}^l$.

The energy consumption of the UD n equipped with a CPU in each computing cycle can be calculated by $\kappa(f_n^l(t))^2$. Similarly, $e_n^l(t)$ represents the energy consumption of local computing tasks:

$$e_n^l(t) = \kappa\beta_n(t)c_n(t)(f_n^l(t))^2 \quad (4)$$

where κ is the effective energy consumption factor depending on the UD n chip architecture.

3.3 Offloading Computing Model

For the offloading computing model, to successfully offload its task offloading to ES, we specify that the minimum and maximum transmission power allocation budgets for each UD n are expressed as p_{min}^l and p_{max}^l (in dBm), respectively. The number of CPUs equipped with each ES m is U_m , the storage capacity constraint is denoted by D_m (in bit), and the computing power per CPU is denoted by f_m^s (in GHz). At the same time, we consider that the wireless transmission channel is a fading model, and the channel changes with different time slot t , but remains constant within the same time slot t . In the user-centric task offloading mode, if a UD n makes an offloading request, when the ES m of its selection accepts the task, the task on the UD n will be passed to the ES m , and the ES m will select a CPU in U_m for task computing. Details are also described in section 4.2.

Similar to the approach in [19], we design to evenly allocate wireless network bandwidth W (in MHz) among K subchannels. For simplicity, the model in this paper makes several assumptions: each wireless transmission subchannel is used exclusively by one UD's tasks at a time, and interference between UDs is not considered.

Additionally, the variance of the channel gain between UD n and ES m is denoted by $h_{n,m}(t)$, and constant noise power σ^2 is assumed, with the noise remaining fixed at a given distance. The normalized channel gain for the uplink channel is then defined as follows:

$$g_{n,m}(t) = \frac{h_{n,m}(t)}{\sigma^2} \quad (5)$$

The transmission of tasks from UD n to ES m requires transmission power, denoted as $p_{n,m}^t(t)$, which is constrained by the transmission power budget of UD n , i.e., $p_{min}^t \leq p_{n,m}^t(t) \leq p_{max}^t$. According to Shannon's capacity theorem, the transmission rate of a single transmission channel in the wireless network is given by $v_{n,m}(t)$, as shown in equation (6):

$$v_{n,m}(t) = \frac{W}{K} \log_2 \left(1 + p_{n,m}^t(t) g_{n,m}(t) \right) \quad (6)$$

Compared to the task data offloaded from UD n to ES m , the data size of computation results returned by ES m is much smaller. Therefore, similar to many other task offloading studies [14,19], we assume that the transmission delay for returning the computation results from ES m to UD n is negligible. Consequently, the transmission delay for offloading the computing task is denoted as $\tau_{n,m}^o(t)$, and it is determined by the transmission rate as follows:

$$\tau_{n,m}^o(t) = \frac{\beta_n(t)}{v_{n,m}(t)} \quad (7)$$

After the UD n task is offloaded to ES m , ES m must process the offloading tasks of all UDs in each time slot. Since the tasks of UD n have deadline constraints, the execution delay of computing tasks on ES m must be carefully considered. Given that U_m is limited and each CPU on ES m can handle only one task at a time, the tasks are processed in order when they arrive, which is determined by the transmission delay $\tau_{n,m}^o(t)$. Based on the arrival order, tasks are assigned to available CPUs in sequence. If no CPU is available when a task arrives, the task must wait until a CPU becomes free. Therefore, we divide the task execution delay on ES m into two parts: the queuing delay while waiting for the earliest available CPU, and the processing delay of the CPU for task computation.

The queuing delay, denoted as $\tau_{n,m}^q(t)$, represents the estimated time before the

earliest executable CPU on ES_m can begin processing the UD_n task. This delay is determined by the completion times of previously accepted offloading tasks on ES_m that arrived before the UD_n task. This approach is adapted from the work of [27]. The processing latency, denoted as $\tau_{n,m}^p(t)$, is determined by the size of UD_n task and the CPU processing power of ES_m :

$$\tau_{n,m}^p(t) = \frac{\beta_n(t)c_n(t)}{f_m^s(t)} \quad (8)$$

Therefore, the total delay of task offloading from the UD_n to the ES_m is expressed as $\tau_{n,m}^a(t)$, which is determined by transmission delay, queuing delay, and processing delay:

$$\tau_{n,m}^a(t) = \tau_{n,m}^p(t) + \max(\tau_{n,m}^o(t), \tau_{n,m}^q(t)) \quad (9)$$

Since the ES in the model is directly powered by the power grid, the energy consumption for the execution of tasks on ES_m is not considered. Instead, we focus only on the energy consumption incurred by UD_n during the offloading process to ES_m . The energy consumption for offloading a computing task is denoted as $e_{n,m}^o(t)$, and is defined as follows:

$$e_{n,m}^o(t) = p_{n,m}^t(t)\tau_{n,m}^o(t) \quad (10)$$

According to the two task calculation models of local and offloading described in Sections 3.2 and 3.3, the total delay and total energy consumption of the UD_n in binary decision mode can be obtained, denoted as $\tau_n(t)$ and $e_n(t)$:

$$\tau_n(t) = (1 - x_n(t))\tau_n^l(t) + x_n(t)\tau_{n,m}^a(t) \quad (11)$$

$$e_n(t) = (1 - x_n(t))e_n^l(t) + x_n(t)e_{n,m}^o(t) \quad (12)$$

3.4 Energy Harvesting Model

For the energy harvesting model, we define the minimum and maximum battery thresholds for each UD_n as b_{min}^h and b_{max}^h (in MJ), respectively. The battery energy is denoted by $b_n(t)$, which is constrained by its power threshold. Energy harvesting work adapted from [14]. Each UD_n is assumed to start fully charged at the beginning of the first time slot, and from then on, energy is harvested at the beginning of each subsequent time slot. The harvested energy is random, denoted as $d_n(t)$. The battery energy is

primarily influenced by the energy consumed through local computation and offloading transmissions. Consequently, the battery energy available in the next time slot depends on both the energy consumed and the energy harvested during the current time slot. The battery energy update rule is governed by the following equation:

$$b_n(t+1) = \min\left(\max\left(b_n(t) - e_n(t) + d_n(t), 0\right), b_{max}^h\right) \quad (13)$$

The battery energy update rule ensures that the battery level of UD n remains within the valid range, meaning it does not drop below zero or exceed the maximum power threshold. For convenience, Table 2 summarizes the key symbols used in the proposed system model.

Table 2 Description of Key Notations Definitions

Notation	Definition
M	Number of edge servers
N	Number of user devices
T	Period of operation
$\varphi_{max}(t)$	Maximum tolerated delay
$\beta_n(t)$	Task byte size of the UD n at time slot t
$c_n(t)$	The number of CPU cycles per bit required by the UD n to process the task
$\varphi_n(t)$	Maximum time deadline for the expected completion of a UD n task
$x_n(t)$	Task offloading decision of the UD n
$y_{n,m}(t)$	Selection decision from the UD n and the ES m
$\tau_n^l(t)$	Local computing delay of the UD n at time slot t
$f_n^l(t)$	Local computing power of the UD n at time slot t
$e_n^l(t)$	Local computing energy consumption of the UD n at time slot t
z_{max}	Maximum user capacity of the ES m
U_m	The number of CPUs the ES m is equipped with
D_m	Maximum storage capacity of the ES m
f_m^s	The CPU power of the ES m
$g_{n,m}(t)$	Normalized channel gain from the UD n to the ES m
$p_{n,m}^t(t)$	Transmission power of the UD n at time slot t
$v_{n,m}(t)$	Channel transmission rate from the UD n to the ES m
$\tau_{n,m}^o(t)$	Offloading computing delay of the UD n at time slot t
$e_{n,m}^o(t)$	Offloading computing energy consumption of the UD n at time slot t
$b_n(t)$	Battery energy of the UD n at time slot t
$d_n(t)$	Energy harvesting by the UD n at time slot t

3.5 Optimization Problem Modeling

According to the system model established in the previous text, each UD must decide whether to offload its tasks to an ES, considering the resource constraints of both the UD and the ES. The goal is to minimize the UD computational cost by reducing both computation delay and energy consumption over the long term. To achieve this, we jointly consider total delay and energy consumption incurred by the UD in a binary decision-making model. We introduce weight coefficients ρ_1 and ρ_2 , which are used to calculate the cost function of the task:

$$C_n(t) = \rho_1 \tau_n(t) + \rho_2 e_n(t) \quad (14)$$

To minimize the average offloading cost across all UDs and run cycles T , we jointly optimize the ES selection decision, task offloading decision, local computing power allocation, and transmission power budget allocation, represented by \mathbf{y} , \mathbf{x} , $\mathbf{f} = \{f_n^l(t) | n \in N, t \in T\}$, and $\mathbf{p} = \{p_{n,m}^t(t) | n \in N, m \in M, t \in T\}$. In summary, the optimization problem P1 is given as follows:

$$\text{P1: } \underset{\mathbf{y}, \mathbf{x}, \mathbf{p}, \mathbf{f}}{\text{minimize}} \quad \frac{1}{T} \sum_{t=1}^T \sum_{n=1}^N C_n(t) \quad (15a)$$

$$\text{s.t.} \quad \sum_{m \in M, N \in N} y_{n,m}(t) = 1, \quad \forall n \in N, \forall m \in M, \forall t \in T \quad (15b)$$

$$x_n(t) \in \{0, 1\}, \quad \forall n \in N, \forall t \in T \quad (15c)$$

$$p_{\min}^t \leq p_{n,m}^t(t) \leq p_{\max}^t, \quad \forall n \in N, \forall m \in M, \forall t \in T \quad (15d)$$

$$f_{\min}^l \leq f_n^l(t) \leq f_{\max}^l, \quad \forall n \in N, \forall t \in T \quad (15e)$$

$$b_{\min}^h \leq b_n^h(t) \leq b_{\max}^h, \quad \forall n \in N, \forall t \in T \quad (15f)$$

$$\varphi_n(t) \leq \varphi_{\max}, \quad \forall n \in N, \forall t \in T \quad (15g)$$

$$z_m(t) \leq z_{\max}, \quad \forall m \in M, \forall t \in T \quad (15h)$$

$$\sum_{n \in Z_m} x_n(t) \leq K, \quad \forall n \in N, \forall m \in M, \forall t \in T \quad (15i)$$

$$\sum_{n \in Z_m} x_n(t) \beta_n(t) \leq D_m, \quad \forall n \in N, \forall m \in M, \forall t \in T \quad (15j)$$

where constraint (15b) ensures that only one ES is selected by each UD for task offloading. (15c) indicates that the task follows a binary decision model, meaning that the task is either offloaded or computed locally. (15d) and (15e) guarantee that the UD

transmission power and local computing capacity remain within their respective allocation budgets. (15f) ensures that the UD's battery energy stays between its minimum and maximum thresholds. (15g) specifies that the computation time for each task must not exceed the specified maximum time limit; otherwise, the task will be discarded. (15h) limits the number of UDs selecting a specific ES to not exceed the ES maximum user capacity. (15i) stipulates that a single subchannel can only be used by one task at any given time, and the number of tasks offloaded to the ES selected by the UD must not exceed the number of available subchannels. Finally, (15j) ensures that the total number of offloaded tasks to the selected ES does not exceed the ES storage capacity.

The optimization problem P1 is a typical non-convex Mixed-Integer Programming (MIP) problem, which is challenging to solve directly due to its NP-hard nature. According to the task model presented in Section 3.1, the offloading decision of the UD is made after selecting the appropriate ES. This implies an inherent coupling between offloading decisions and server selection. To simplify the problem, the original optimization problem P1 is decomposed into two subproblems: one focused on the selection decision between the user and the server, and the other on the offloading decision. The optimization problem P2, which addresses the selection decision between the user and the server, is formulated as follows:

$$\text{P2: } \underset{\mathbf{y}}{\text{minimize}} \quad \frac{1}{T} \sum_{t=1}^T \sum_{n=1}^N C_n(t) \quad (16a)$$

$$\text{s.t.} \quad \sum_{m \in M, N \in N} y_{n,m}(t) = 1, \quad \forall n \in N, \forall m \in M, \forall t \in T \quad (16b)$$

$$z_m(t) \leq z_{max}, \quad \forall m \in M, \forall t \in T \quad (16c)$$

After obtaining selection decision \mathbf{y} from optimization problem P2, we bring it into optimization problem P1, and we get offloading decision optimization problem P3 as shown below:

$$\text{P3: } \underset{\mathbf{x}, \mathbf{p}, \mathbf{f}}{\text{minimize}} \quad \frac{1}{T} \sum_{t=1}^T \sum_{n=1}^N C_n(t) \quad (17a)$$

$$\text{s.t.} \quad x_n(t) \in \{0, 1\}, \quad \forall n \in N, \forall t \in T \quad (17b)$$

$$p_{min}^t \leq p_{n,m}^t(t) \leq p_{max}^t, \quad \forall n \in N, \forall m \in M, \forall t \in T \quad (17c)$$

$$f_{min}^l \leq f_n^l(t) \leq f_{max}^l, \quad \forall n \in N, \forall t \in T \quad (17d)$$

$$b_{min}^h \leq b_n^h(t) \leq b_{max}^h, \quad \forall n \in N, \forall t \in T \quad (17e)$$

$$\varphi_n(t) \leq \varphi_{max}, \quad \forall n \in N, \forall t \in T \quad (17f)$$

$$\sum_{n \in Z_m} x_n(t) \leq K, \quad \forall n \in N, \forall m \in M, \forall t \in T \quad (17g)$$

$$\sum_{n \in Z_m} x_n(t) \beta_n(t) \leq D_m, \quad \forall n \in N, \forall m \in M, \forall t \in T \quad (17h)$$

4 User-centric DRL Model Splitting Inference Scheme

To address the optimization problem P1 presented in Section 3, we propose a user-centric DRL-based model splitting and inference scheme. we propose a user-centric DRL model splitting inference scheme and a UCMS_MADDPG-based offloading algorithm. This transforms the problem of minimizing costs into a problem of maximizing returns. The proposed scheme proceeds as follows: First, a user-server co-selection algorithm is applied to address the matching and selection process between the UD and ES. Following this, the UCMS_MADDPG algorithm is employed to jointly optimize offloading decisions, local computing power allocation, and transmission power budgeting for each UD, determining the optimal offloading strategy.

4.1 User-server Co-selection Algorithm

In the ES selection phase of traditional algorithms, the UD often preferentially selects the ES with maximum channel gain for task offloading. Since the user capacity and storage capacity of the ES is considered in our system, the traditional algorithm may cause a part of the ES in the system to be overloaded and tasks will be easily lost. This incurs a high offloading cost. However, due to the underutilization of other ES, a lot of computing resources are wasted. In order to obtain a better selection strategy, we propose a co-selection algorithm. It makes the UD and the ES make decisions together in the direction of maximizing their own interests, and achieves high resource utilization. To implement the algorithm, we define the selection function to quantify the respective benefits of the UD and the ES.

From the point of view of the UD, the primary objective is to minimize its own computation delay and energy consumption. When selecting the target ES, the UD will preferentially select the ES offloading tasks with a faster transmission rate, shorter execution delay, and more abundant remaining computing resources. Consequently, the

total offloading delay and offloading energy consumption can be directly determined. Then the selection function of UD n is expressed as $I_m(t)$ and the following equality is satisfied:

$$I_m(t) = \sum_{n \in Z_m} (\rho_1 \tau_{n,m}^a(t) + \rho_2 e_{n,m}^o(t)), m \in M \quad (18)$$

From the ES's perspective, its objective is also to minimize computation delay. Therefore, the ES will prioritize UD s with smaller computation tasks to complete the processing more quickly. The selection function of ES m is denoted as $I_n(t)$ and the corresponding equality is defined as follows:

$$I_n(t) = \tau_{n,m}^a(t), n \in N \quad (19)$$

The user-server co-selection algorithm is mainly determined according to the selection function and the user capacity of the ES, and the specific implementation is shown in Algorithm 1.

Algorithm 1: User-server Co-selection Algorithm

Input: $I_m(t)$, $I_n(t)$, z_{max}

Output: $y_{n,m}(t)$, Z_m

- 1: Initialize the UD set N , the ES set M , the rejection list $N^r(t) = N$, and initialize the application list $N_{n,m}^a(t)$
- 2: **for** each ES m **do**
- 3: Initialize the selection list $Z_m(t)$, user capacity $z_m(t)$
- 4: **end for**
- 5: **while** $N^r(t) > 0$ **do**
- 6: **for** each UD $n \in N^r(t)$ **do**
- 7: **if** $0 < z_m(t) \leq z_{max}$ of the ES m **then**
- 8: Sort the selection function values of all ES m in ascending order
- 9: Send the request to the ES m with the lowest selection function value
- 10: Update application list $N_{n,m}^a(t)$
- 11: **else**
- 12: **break**
- 13: **end for**
- 14: **for** each ES m **do**
- 15: **if** $z_m(t) = z_{max}$ of the ES m **then**
- 16: Skip the ES m
- 17: Sort the selection function values of all UD n in $N_{n,m}^a(t)$ in ascending order
- 18: **for** each UD n after sorting **do**

```

20:             if  $z_m(t) < z_{max}$  of the  $ES_m$  then
21:                 The  $UD_n$  is selected by the  $ES_m$ 
22:                 Updating selection list  $Z_m(t) = Z_m(t) + UD_n$ 
23:                 Updating rejection list  $N^r(t) = N^r(t) - UD_n$ 
24:             else
25:                 break
26:             end for
27:         Clear application list  $N_{n,m}^a(t)$ 
28:         Update the user capacity of the  $ES_m$   $z_m(t) = z_m(t) + UD_n$ 
29:     end for
30: end while

```

First, the rejection list $N^r(t)$ is created, and all UD's are added to it. An initialized application list $N_{n,m}^a(t)$ is used to track each UD's application to the ES, while the selection list $Z_m(t)$ for each ES is initialized to store the connected UD's and track user capacity $z_m(t)$. The algorithm then enters an iterative process. In each iteration, sort unselected UD's in ascending order based on ES selection function $I_n(t)$, with priority given to sending the application to the ES with the lowest function value. Upon receiving application of UD, each ES is sorted in ascending order according to the UD selection function $I_m(t)$, prioritizing UD's with lower function values until the user capacity of ES reaches its upper limit. The selected UD is added to the selection list, while the requests from remaining UD's are rejected. After each selection round, the ES clears its application list and updates its remaining user capacity. The iteration ends when there are no UD's left in the rejection list; otherwise, the process continues until all UD's in the rejection list are assigned to the appropriate ES.

4.2 MDP Formulation

DRL is based on the Markov Decision Process (MDP). Before designing DRL algorithms, the research problem must be modeled and converted into an MDP framework. To solve the optimization problem P2 in Section 3.5, this section models the task offloading decision \mathbf{x} , local computing power allocation \mathbf{f} , and transmission power budget allocation \mathbf{p} of the UD as an MDP. The three key components of the MDP

are described in detail below.

4.2.1 State

In time slot t of the system environment, the current state is obtained by the set of UDn task $(\beta_n(t), c_n(t), \varphi_n(t))$, local computing power $f_n^l(t)$, offloading transmission power $p_{n,m}^t(t)$, battery energy $b_n(t)$, and normalized channel gain $g_{n,m}(t)$ between UDn and each edge server ESm. This state is expressed as $S_n(t)$:

$$S_n(t) = \{s_n^t(t), s_n^f(t), s_n^p(t), s_n^b(t), s_n^g(t)\} \in S(t) \quad (20)$$

where task state $s_n^t(t) = (\beta_n(t), c_n(t), \varphi_n(t))$, local computing power state $s_n^f(t) = f_n^l(t)$, offloading transmission power state $s_n^p(t) = p_{n,m}^t(t)$, battery energy state $s_n^b(t) = b_n(t)$, and normalized channel gain state $s_n^g(t) = g_{n,m}(t)$.

4.2.2 Action

In time slot t , there are three decision variables for the system's computing tasks: the binary offloading decision $x_n(t)$, local computing power allocation $f_n^l(t)$, and transmission power allocation $p_{n,m}^t(t)$. In the user-centric model splitting inference scheme, the UDn first calculates the corresponding offloading pre-decision and resource allocation for its CPU, then transmits its status and action information to the selected edge server ESm. The ESm then uses its CPU to calculate the offloading pre-decision. The execution process is as follows:

(1) For a UDn that makes a local computing decision, the ESm respects this decision.

(2) For a UDn that makes an offloading computing decision, the ESm makes a hybrid decision based on the recommendation of the UDn and its resources.

(3) If the number of UDn requesting offloading exceeds the available subchannels of ESm, or if the total size of the offloaded tasks surpasses the storage capacity of ESm, the ESm will decide which the UDn to approve based on a hybrid decision.

(4) If the sum of the number of UDn proposed offloading and their task sizes are less than the resource constraints of the ESm, the ESm accepts applications from all UDn. The task is then assigned to the subchannel and the task offloading computing

begins.

The entire action space is denoted as $A(t)$ and is split into two distinct components: the UD action and the ES action. Each UD n generates three actions between $[0,1]$ for offloading pre-decisions and resource allocation in time slot t . The set of these actions constitutes the UD action, represented as $A_u(t)$:

$$A_u(t) = \{x_n^u(t), f_n^u(t), p_{n,m}^u(t)\} \quad (21)$$

where $x_n^u(t)$ is the task offloading pre-decision action of the UD n . If $x_n^u(t) < 0.5$, let $x_n(t) = 0$ in equation (1). Otherwise, it is transmitted to the ES m for hybrid decision. The local computing power allocation $f_n^l(t)$ is calculated according to the $f_n^u(t)$ action, as shown in equation (22). Similarly, the transmission power allocation $p_{n,m}^t(t)$ is calculated according to the action $p_{n,m}^u(t)$, as shown in equation (23).

$$f_n^l(t) = \max(f_{min}^l, f_n^u(t) f_{max}^l) \quad (22)$$

$$p_n^t(t) = \max(p_{min}^t, p_{n,m}^u(t) p_{max}^t) \quad (23)$$

For a UD n whose value is $x_n^u(t) \geq 0.5$, the UD n submits an offloading request to the ES m whose connection is successfully selected. After obtaining its status and action information, the ES m makes a binary hybrid decision. The hybrid decision determines which UD n applications are approved. The ES action is denoted by $A_m(t)$, as follows:

$$A_m(t) = \{x_n^m(t)\} \quad (24)$$

where let $x_n(t) = 1$ for the UD n of consent application and $x_n(t) = 0$ otherwise.

4.2.3 Reward

After the UD n executes the action, the system environment is updated, and reward feedback is obtained. The reward function is crucial in DRL, so it is important to fully consider the constraints in the optimization problem. While other constraints for the UD and ES have been addressed in previous works, here we focus on the task time and battery energy constraints. We use the inverse of the cost function from Section 3.5 as the reward term, and the task time and battery energy limits of UD n as the penalty term.

In [14], the reward for battery depletion included a drop penalty. In this paper, we define that the penalty starts when the specified minimum power threshold is exceeded.

The penalty function is denoted as $P_n(t)$ and satisfies the following:

$$P_n(t) = \rho_1 \min((\varphi_n(t) - \tau_n(t)), 0) + \rho_2 \min((b_n(t) - b_{min}^h), 0) \quad (25)$$

Therefore, the reward function of each UD n within the shared time slot t is defined as $r_n(t)$:

$$r_n(t) = -\left(\frac{1}{N} \sum_{n=1}^N C_n(t) + P_n(t)\right) \quad (26)$$

4.3 UCMS_MADDPG-based Offloading Algorithm

According to the MDP transformation model in Section 4.2, this chapter proposes an offloading algorithm using UCMS_MADDPG. The algorithm is designed on the actor-critic framework of the MADDPG algorithm, combined with DQN. In the AIoT multi-edge server deployment environment, each UD n is treated as an agent. The policy network of each agent takes the local state as input, while the Q-network takes the global state and the set of actions from all agents as input. Additionally, we introduce a priority sampling mechanism for reward error trade-off, which determines the priority of samples during the experience replay process more effectively.

Fig. 3. shows the architecture diagram of the UCMS_MADDPG-based offloading algorithm. After the UD n generates the output, the following operations will be performed: if $x_n^u(t) < 0.5$, let $x_n(t) = 0$, and start the local computation. Otherwise, it transmits $x_n^u(t), f_n^u(t), p_{n,m}^u(t)$ to the ES m for hybrid decision. Subsequently, the ES m produces binary decisions and feeds them back to the UD n . Finally, the reward within the shared time slot t is calculated and provided to the ES m for training. The UD n is trained using a trade-off value of reward and TD error computed by the ES m .

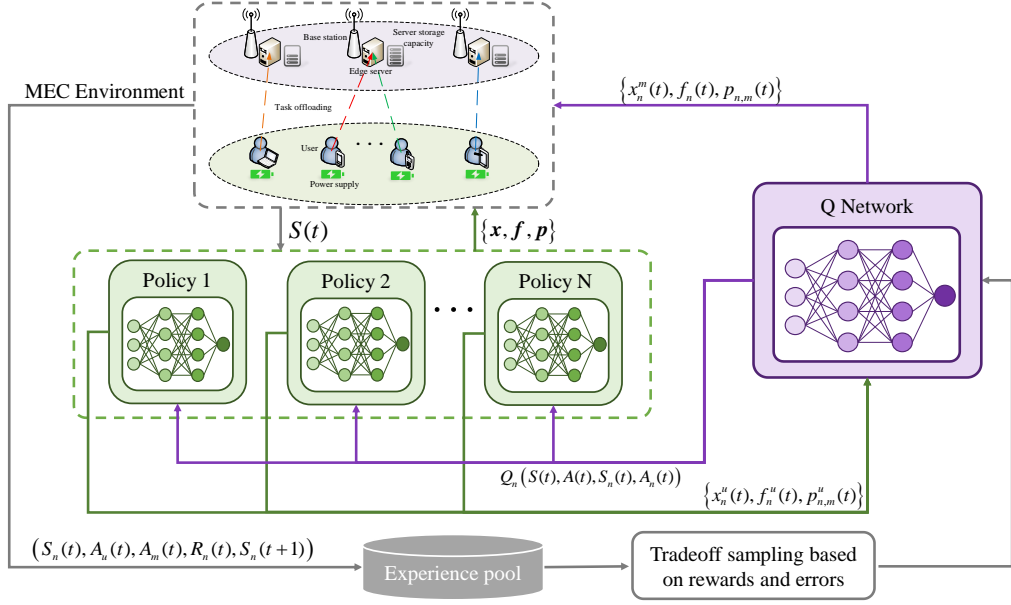


Fig.3 Offloading algorithm architecture based on UCMS_MADDPG

4.3.1 Preferential Sampling Mechanism of Reward Error Trade-off

In the experience replay process, the existing preferential sampling mechanism typically uses the TD error as an index to measure the importance of experience samples. However, due to the continuous update of neural network parameters, the TD error changes dynamically. As a result, some samples with gradually decreasing TD errors may still be selected with high probability for training the Q-network. This can lead to overfitting, causing the agent to focus too much on these samples and potentially fall into a local optimum, which negatively impacts the global optimization of the policy. To address this issue, we propose using a trade-off between the current reward and the TD error to update the sampling priority of experience samples. This composite priority mechanism effectively balances short-term feedback and long-term error, improving the diversity of experience replay and enhancing training robustness. Ultimately, it helps the agent escape local optima and achieve better policy performance.

So we use trade-off value of current reward $r_n(t)$ and TD error $\delta_n(t)$ to calculate the composite priority of experience samples, denoted as $\eta(t)$. Firstly, $\eta_r(t)$ is defined as the priority based on the current reward and $\eta_\delta(t)$ is defined as the priority based on the TD error, which satisfies the following two equalities.

$$\eta_r(t) = |r_n(t)| + \varepsilon \quad (27)$$

$$\eta_\delta(t) = |\delta_n(t)| + \varepsilon \quad (28)$$

Define ν_r and ν_δ as the trade-off factors of $\eta_r(t)$ and $\eta_\delta(t)$ respectively, and satisfy $\nu_r + \nu_\delta = 1$, then the compound priority $\eta(t)$ is calculated as follows:

$$\eta(t) = \nu_r \eta_r(t) + \nu_\delta \eta_\delta(t) \quad (29)$$

Assuming that the set of experience samples selected in each batch is B and the number of experience samples selected is N_B , the sampling probability of experience samples in Article i ($i \leq N_B$) is represented by $p_i^B(t)$:

$$p_i^B(t) = \frac{\eta_i(t)}{\sum_{i \in B} \eta_i(t)} \quad (30)$$

4.3.2 Policy Updates

Since the objective of this paper is to design an offloading algorithm that maximizes the UD's returns over a continuous period, it must consider both immediate rewards and long-term cumulative returns using Bellman's equation. Given the immediate reward $R_n(t) = r_n(S(t), A(t))$, the Q function satisfies the following:

$$Q_n(S(t), A(t), S_n(t), A_n(t)) = \mathbb{E} \left[R_n(t) + \gamma P_n(S(t+1)) \max_{S_n(t+1), A_n(t+1)} Q_n(S(t+1), A(t+1), S_n(t+1), A_n(t+1)) \right] \quad (31)$$

where γ is discount factor, $S(t)$, $A(t)$ and $S(t+1)$, $A(t+1)$ are the set of the current state, action and the next state, action of all UD n that select the ESm. $S_n(t)$, $A_n(t)$ and $S_n(t+1)$, $A_n(t+1)$ are the set of the current state, action and the next state, action of all UD n in the hybrid decision of the ESm.

In the training of UCMS_MADDPG-based offloading algorithm, UD and ES have different Q networks and policy networks respectively. However, since ES actions are discrete and determined based on the calculation of relative Q values of tasks, ES does not need an explicit policy network to generate actions. We define that UD action $A_u(t)$ mentioned in Section 4.2.2 follows directly from current state $S_n(t)$, i.e., $A_u(t) \leftarrow \lambda(S_n(t))$, where λ is a policy parameter of the UD. ES action $A_m(t)$ is derived based on the UD action, i.e., $A_m(t) \leftarrow \theta(S(t), A(t), S_u(t), A_u(t))$, where $S(t)$

is the set of states of all UD n that select this ES m , $A(t)$ is the set of actions, and similarly, $S_u(t)$ and $A_u(t)$ are the set of states and actions of all UD n with $x_n^u(t) \geq 0.5$, and θ is policy parameter of all ESs.

In both ES and UD, a mini-batch of data B ($i \in B$) is randomly sampled from the experience pool of the preferential sampling mechanism of reward error trade-off. First, training on ES learns offloading strategy by maximizing the global reward, and uses target Q network $Q'_{i,m}$ to calculate target Q value, which is represented by $y_i(t)$:

$$y_i(t) = R_i(t) + \gamma \max_{S_{i,n}(t+1), A_{i,n}(t+1)} Q'_{i,m}(t+1) \quad (32)$$

Then, the loss function of Q network $Q_{i,m}$ is defined according to the Weighted mean square error (Weighted MSE), and the loss function is defined as $L(Q_{i,m})$:

$$L(Q_{i,m}) = \mathbb{E} \left[\eta(t) (y_i(t) - Q_{i,m}(t))^2 \right] \quad (33)$$

And update Q network parameter $\theta_{Q_{i,m}}$ as $\theta_{Q_{i,m}} \leftarrow \theta_{Q_{i,m}} - \alpha_Q \nabla_{\theta_{Q_{i,m}}} L(Q_{i,m})$, where α_Q is Q network learning rate. To improve the stability of network training, soft update mechanism is used to synchronize the parameters $\theta_{Q'_{i,m}} \leftarrow \omega \theta_{Q_{i,m}} + (1-\omega) \theta_{Q'_{i,m}}$ of the target Q network $Q'_{i,m}$, where ω is the target network update coefficient.

Training for the UD includes the optimization of Q networks and policy networks to generate efficient offloading decisions. For each training sample, the UD relies on the target Q value provided by the ES to perform its own Q network update and policy optimization, thus ensuring that the global policy optimization proceeds in a consistent direction. Specifically, the UD first obtains the optimization objective from the target Q value provided by ES and computes its own Q network loss function. The loss function of the Q network $Q_{i,u}$ of UD is defined as $L(Q_{i,u})$:

$$L(Q_{i,u}) = \mathbb{E} \left[\eta(t) (y_i(t) - Q_{i,u}(t))^2 \right] \quad (34)$$

And update the Q network parameter $\lambda_{Q_{i,u}}$ as $\lambda_{Q_{i,u}} \leftarrow \lambda_{Q_{i,u}} - \alpha_Q \nabla_{\lambda_{Q_{i,u}}} L(Q_{i,u})$. The gradient of the policy network μ_u is then calculated using the current target Q value, denoted by $\nabla_{\lambda_{\mu_u}} J(\mu_u)$:

$$\nabla_{\lambda_{\mu_u}} J(\mu_n) = \mathbb{E} \left[\nabla_{\lambda_{\mu_u}} \mu_u(S_i(t)) \nabla_{A_{i,n}(t)} Q_i(t) \right] \quad (35)$$

Then update the policy network parameter $\lambda_{\mu_u} \leftarrow \lambda_{\mu_u} + \alpha_{\mu} \nabla_{\lambda_{\mu_u}} J(\mu_u)$ of the UD, where α_{μ} is the policy network learning rate. Finally, the target network $Q'_{i,u}$ and the target policy network μ'_n are soft updated $\lambda_{Q'_{i,u}} \leftarrow \omega \lambda_{Q_{i,u}} + (1-\omega) \lambda_{Q'_{i,u}}$, $\lambda_{\mu'_u} \leftarrow \omega \lambda_{\mu_u} + (1-\omega) \lambda_{\mu'_u}$.

In summary, the specific steps of UCMS_MADDPG-based offloading algorithm are shown in Algorithm 2.

Algorithm 2: UCMS_MADDPG-based Offloading Algorithm

Input: Maximum number of rounds Ep_{max} , Number of training rounds Ep_{train}

Output: $x_n(t)$, $f_n^l(t)$, $p'_{n,m}(t)$

```

1:   while  $Ep_{now} < Ep_{max}$  do
2:       Execute the reset() method to reset the system environment
3:       Get the initial state of the current environment  $S_n(t)$ 
4:       for  $t = 1 \dots T$  do
5:           for each UD $n$  do
6:               Obtain offloading action based on local status  $A_u(t), A_m(t)$ 
7:           end for
8:           Get the reward  $R_n(t)$ , and the next state  $S_n(t+1)$ 
9:           Save  $(S_n(t), A_u(t), A_m(t), R_n(t), S_n(t+1))$  to the experience replay buffer
10:          Execute the step() method to update the state  $S_n(t) \leftarrow S_n(t+1)$ 
11:         end for
12:        for  $Ep_{train}$  do
13:            The set of experience samples collected from the experience replay buffer is B
14:            Extract the data  $(S_n(t), A_u(t), A_m(t), R_n(t), S_n(t+1))$  of each batch sample B
15:            for each UD $n$  do
16:                The goal policy network is used to calculate the next goal action  $A_u(t+1)$ 
17:            end for
18:            for B do
19:                if  $x_n^m(t) = 1$  then
20:                    Execute Equation (32) to calculate the target Q value  $y_i(t)$ 
21:                else if  $x_n^m(t) = 0$  then
22:                    The default Q value is computed using zero states and actions
23:                end if
24:                Update the current Q value of the Q network
25:                Cumulative reward error trade-off values for prioritized experience replay

```

```

26:         end for
27:         Execute Equation (33) to calculate the Q network loss  $L(Q_{i,m})$ 
28:         Update the Q network parameters  $\theta_{Q_{i,m}}$ 
29:         Soft update target Q network parameters  $\theta'_{Q_{i,m}}$ 
30:         for each UD $n$  do
31:             Generate new actions using a policy network  $A_u(t)$ 
32:             Calculate Q value related to new actions using the Q network of the ES
33:             Execute Equation(34) to calculate Q network loss  $L(Q_{i,u})$ , and update  $\lambda_{Q_{i,u}}$ 
34:             Execute Equation(35) to calculate policy network gradient  $\nabla_{\lambda_{\mu_u}} J(\mu_u)$ , and
35:             update  $\lambda_{\mu_u}$ 
36:             Soft update target Q network  $\lambda'_{Q_{i,u}}$ , and target policy network  $\lambda'_{\mu_u}$ 
37:         end for
38:         Update the sampling weights of samples based on the composite priority  $\eta(t)$ 
39:     end while

```

5 Simulation Results and Analysis

5.1 Simulation Parameter Setting

In the AIoT multi-edge server deployment dynamic MEC environment established above, the number of UD N is set to 48, and the number of MEC servers M is set to 3. The parameter settings from references [14,19] were used to construct the experimental environment for this paper. All UDs have identical local computing capacity, transmission power allocation, and battery threshold. While modern ESs typically have storage capacities of several GB or more, we chose a smaller value to simulate high-voltage conditions, setting the server storage capacity to 400 MB. Specific parameter settings are provided in Table 3.

The proposed UCMS_MADDPG algorithm is implemented using the PyTorch framework. Simulations were conducted with Python 3.9 and PyTorch 2.2 on a host machine equipped with an NVIDIA GeForce RTX 4070 GPU and a 13th Gen Intel Core i5-13600KF CPU (runs at 3.5GHz and 32GB RAM). The strategy network and Q network are both composed of two fully connected layers, with 64 and 512 neurons, respectively. And set the learning rate of policy network and Q network as $1 \times e^{-4}$ and

$1 \times e^{-3}$ respectively, the number of experience samples in each batch of training N_B is 64, the capacity of the experience buffer pool is $1 \times e^5$, the discount coefficient is 0.99, and the Adam optimizer is used for gradient descent calculation during training.

Table 3 System Parameter Setting

Parameter	Value
The number of edge servers M	3
The number of user devices N	48
Maximum tolerated delay $\varphi_{max}(t)$	[0.1,1] s
Task size in bytes $\beta_n(t)$	[1-50] MB
The number of CPU cycles per bit required by the task $c_n(t)$	[300,700] cycles/bit
Maximum local computing capacity f_{max}^l	1.5 GHz
Minimum local computing power f_{min}^l	0.4 GHz
Maximum transmission power p_{max}^t	24 dBm
Minimum transmission power p_{min}^t	1 dBm
Maximum battery threshold b_{max}^h	3.2 MJ
Minimum battery threshold b_{min}^h	0.5 MJ
Maximum user capacity z_{max}	16
The number of CPUs equipped U_m	8
Maximum storage capacity D_m	400 MB
Server CPU computing power f_m^s	4 GHz
Normalized channel gain $g_{n,m}(t)$	[5,14] dB
Energy consumption factor κ	$5 \times e^{-27}$
Wireless Network bandwidth W	40 MHz
The number of subchannels K	10
Harvested energy $d_n(t)$	$1 \times e^{-3}$ J
Cost weight coefficient ρ_1	0.5
Cost weight coefficient ρ_2	0.5

5.2 Baseline Comparison Scheme

To assess the performance of the UCMS_MADDPG algorithm, we compare it against several benchmark algorithms based on MADDPG through simulation experiments:

- RD_UCMS_MADDPG: Only the UCMS_MADDPG algorithm is used to optimize resource and offloading decisions, random selection is made between the user and the server, and no co-selection algorithm is used.

- MADDPG: Extends the DDPG algorithm by using centralized policy evaluation and decentralized policy execution, allowing multiple agents to learn collaboratively. When the policy is updated, the Q network is used to master the global information to guide the policy network for training. When interacting with the environment, the policy network generates actions only by acquiring local states.
- OFFLOADCOST_MADDPG: A heuristic MADDPG algorithm with minimum offloading cost first. By calculating and ranking the combined cost of each task, the solution with the smallest offloading cost is selected as the priority.
- DEADLINE_MADDPG: A heuristic MADDPG algorithm with a deadline first. By calculating and sorting the deadline of each task, the alternative closest to the deadline is selected as the priority.

5.3 Algorithms Performance Analysis

First, we set 2000 training sets, each containing 10 time slots, and conducted the experiment 10 times to generate the results. Fig. 4. shows the convergence comparison between UCMS_MADDPG and RD_UCMS_MADDPG in the training environment. Initially, the reward values for both algorithms are relatively low. However, as training progresses, the reward values increase and eventually stabilize at higher levels. It can be seen that UCMS-MADDPG has a faster convergence speed and gradually converges around 60 rounds of training, indicating that the UCMS-MADDPG network has been effectively trained. In contrast, RD_UCMS_MADDPG converges more slowly, with a lower overall system return compared to UCMS_MADDPG.

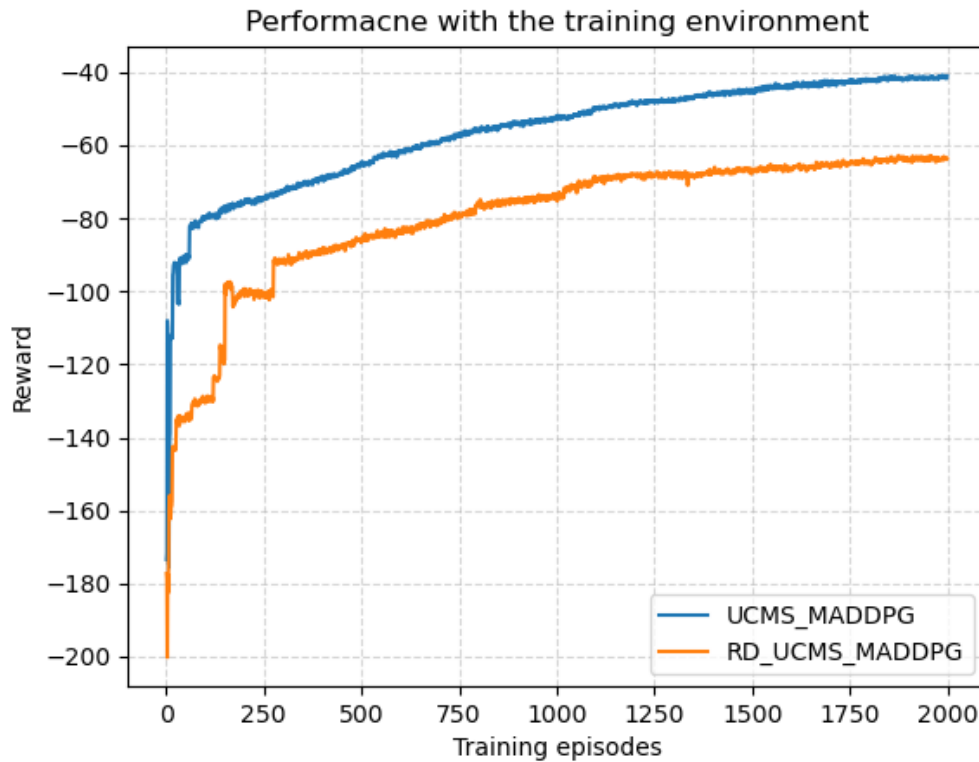


Fig.4 Comparison of convergence performance in the training environment

Fig. 5. shows the performance comparison between UCMS_MADDPG and four baseline methods: RD_UCMS_MADDPG, MADDPG, OFFLOADCOST_MADDPG, and DEADLINE_MADDPG. It is evident that UCMS_MADDPG outperforms all other methods, effectively utilizing global information and avoiding local optima. RD_UCMS_MADDPG exhibits larger reward fluctuations and lower reward values, suggesting that random user-server selection is not suitable for dynamic offloading scenarios. MADDPG consistently produces lower average rewards, as it relies solely on the actor to analyze global information, with the critic only providing feedback. This structure leads to longer convergence times in complex environments. In contrast, OFFLOADCOST_MADDPG and DEADLINE_MADDPG introduce artificial priority rules, which improve early-stage efficiency. However, these rules reduce the algorithm's flexibility, causing them to perform worse than UCMS_MADDPG in dynamic task and resource environments, and leading to local optima early in training. While they achieve better returns than MADDPG, they require more rounds to converge.

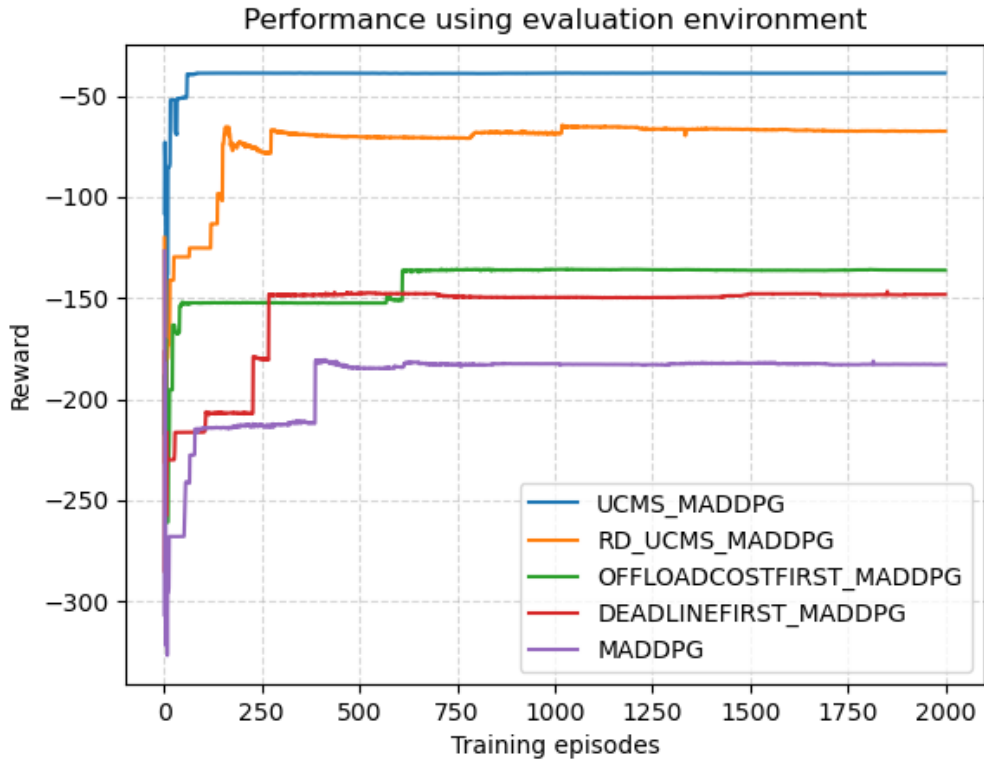


Fig.5 Performance comparison for different algorithms in the evaluation environment

To further evaluate the performance of UCMS_MADDPG-based offloading algorithm, we compare the performance of UCMS_MADDPG with the four benchmark algorithms in terms of total system cost as the number of UDs increases from 12 to 57, as illustrated in Fig. 6. As the number of UDs grows, the ES load increases, leading to a decrease in available computation and communication resources per UD, which results in a significant rise in total cost. Overall, MADDPG incurs the highest total cost, followed by OFFLOADCOST_MADDPG and DEADLINE_MADDPG, while UCMS_MADDPG consistently maintains the lowest total system cost. This demonstrates the superior adaptability of UCMS_MADDPG in high-load offloading scenarios.

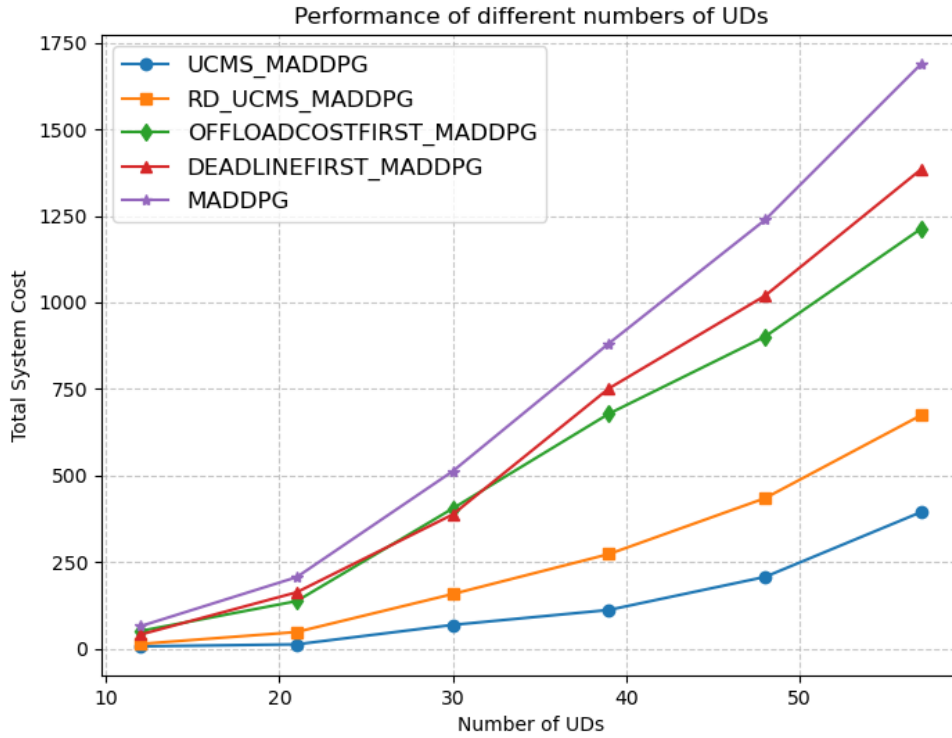


Fig.6 Comparison of total system cost with different numbers of the UD

Then further compare the performance of UCMS_MADDPG with the four benchmark algorithms in terms of server participation decisions. To reduce the complexity of image information, we apply the Savitzky-Golay filter to smooth the data and down-sample every 100 rounds, as shown in Fig. 7. The figure reveals that UCMS_MADDPG maintains a higher server participation rate, which correlates with its lower total system cost. In contrast, MADDPG and the two heuristic algorithms show a high server participation rate initially, but this rate gradually decreases with each iteration and eventually stabilizes at a low level. This suggests that MADDPG, when used alone, struggles to effectively adapt to the complexities of resource competition and task allocation in dynamic scenarios.

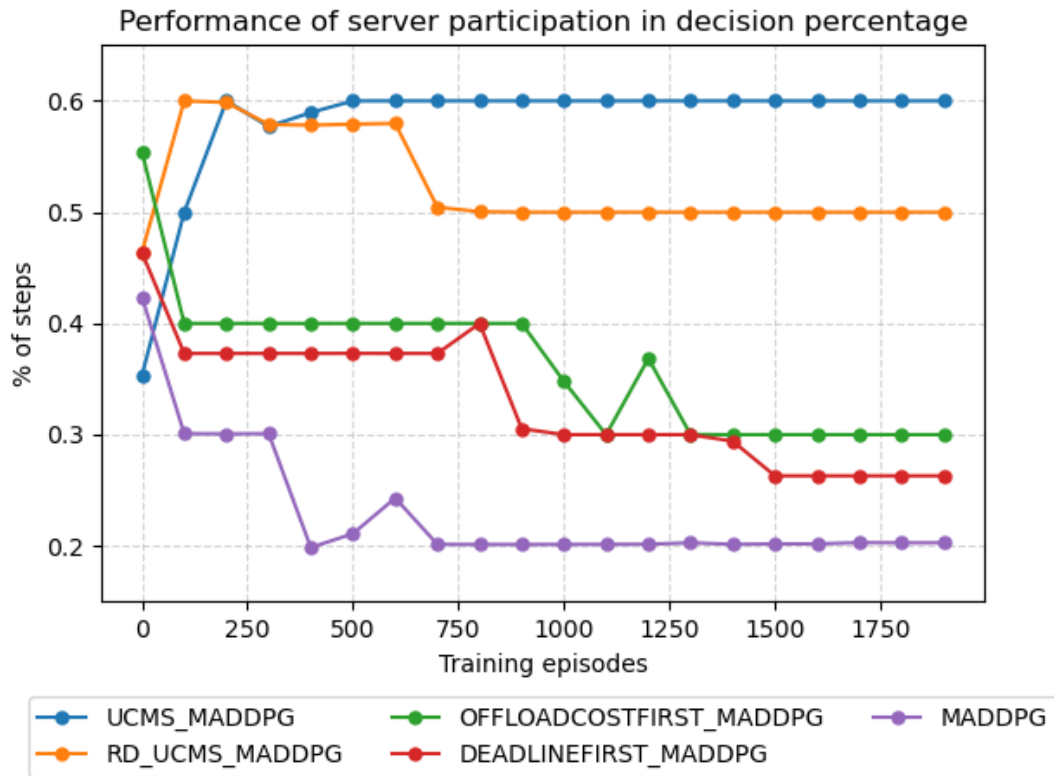


Fig.7 Percentage of servers participating in decision for different algorithms

Similarly, Fig. 8. compares the performance of UCMS_MADDPG with the four benchmark algorithms in terms of task timeouts. UCMS_MADDPG demonstrates a significantly lower percentage of task timeouts during offloading compared to the other algorithms. However, the plot in Fig. 8. resembles a vertically flipped version of Fig. 5., indicating that time delay plays a dominant role in the overall system cost. This suggests that the weight coefficient $\rho_1 = \rho_2 = 0.5$ does not effectively balance delay and energy consumption.

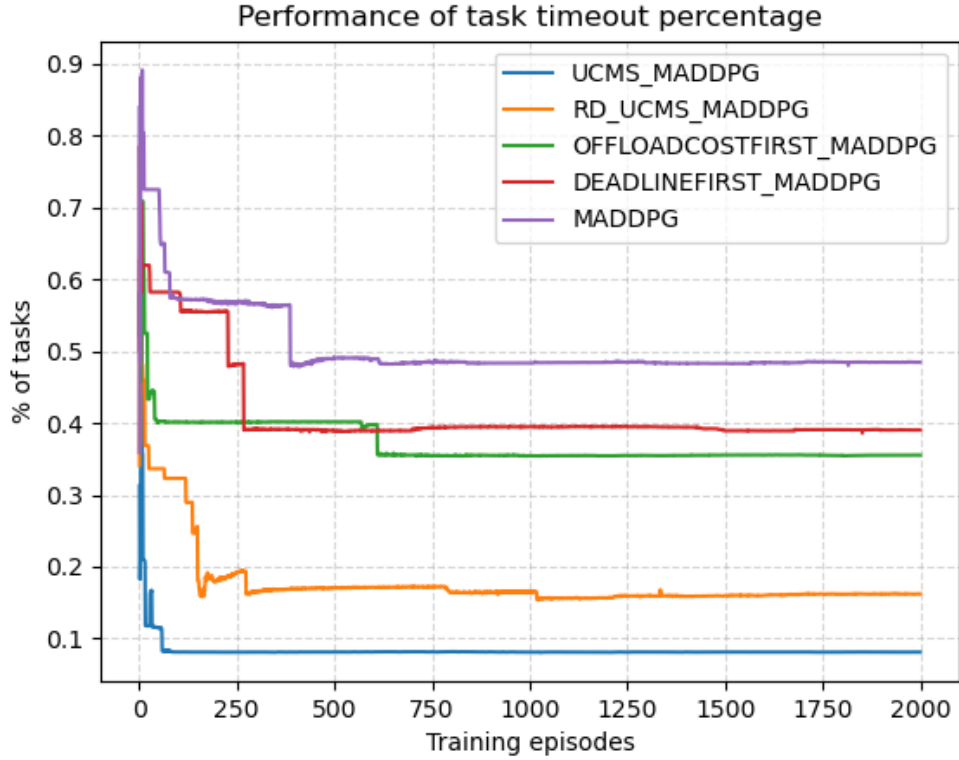


Fig.8 Percentage of task timeouts for different algorithms

To further assess the impact of energy consumption, we set the maximum battery threshold b_{max}^h to 1J to increase the energy consumption penalty. The weight coefficients $\rho_1=1$ and $\rho_2=5$ are adjusted to amplify the importance of energy consumption. Additionally, the time slot of each episode is extended to 100 to improve the test performance. Fig. 9. shows the performance comparison of different algorithms with 100 time slots per episode. It can be observed that UCMS_MADDPG still achieves optimal performance. In contrast to the experiment with 10 time slots, MADDPG and the heuristic algorithms perform closer to UCMS_MADDPG with 100 time slots. This improvement is due to the increased number of time slots, which generates more empirical data, allowing the algorithm to generalize better.

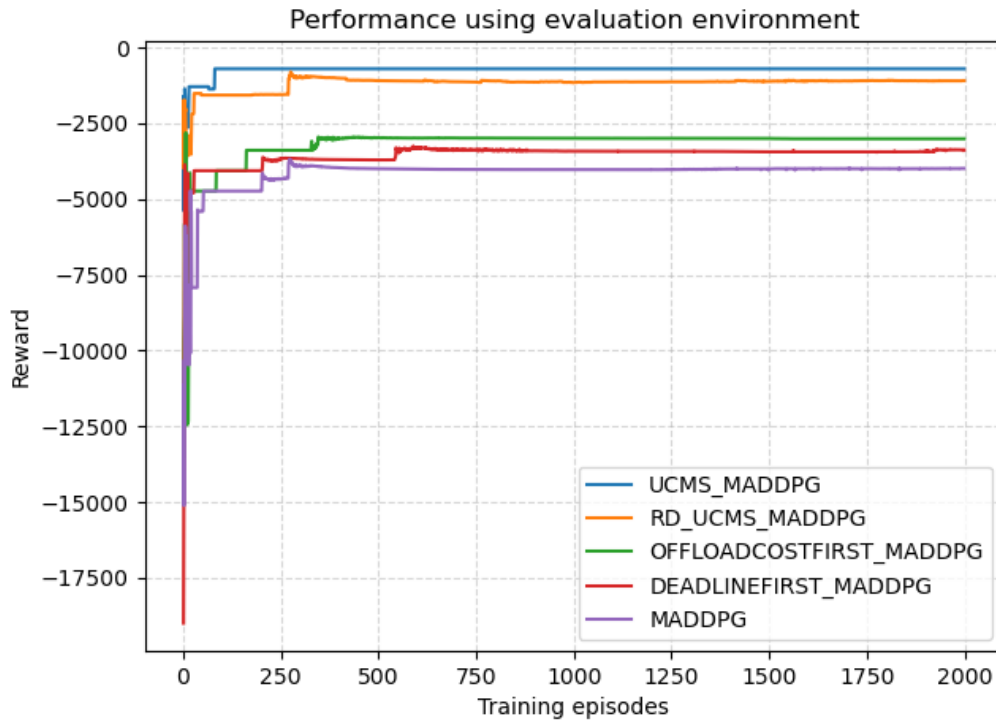


Fig.9 Performance comparison for different algorithms in 100 time slots

Similarly, Fig. 10. illustrates the task timeout percentages for different algorithms with 100 time slots. There are significant differences between Fig. 10. and Fig. 9., indicating that the modification of experimental parameters has played a role. Next, we will observe the impact of energy consumption and compare the performance of UCMS_MADDPG and the other four benchmark algorithms in exceeding the battery threshold. The percentage of different algorithms below the battery threshold is shown in Fig. 11. It can be observed that UCMS_MADDPG performs similarly to the other baseline algorithms in this regard, as the overall system return considers the sum of latency and energy consumption, while Fig. 11. only shows the number of UDs running below the battery threshold. According to the other experimental results, it can be concluded that UCMS_MADDPG has better overall performance, and greater advantages in dynamic environments.

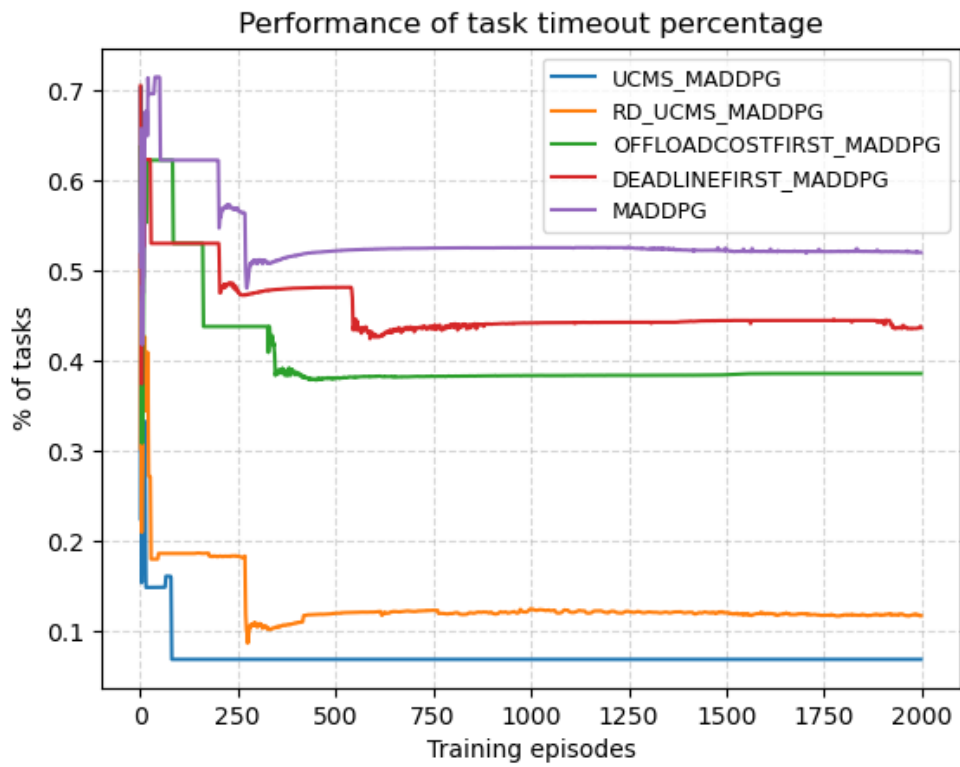


Fig.10 Percentage of task timeouts for different algorithms in 100 time slots

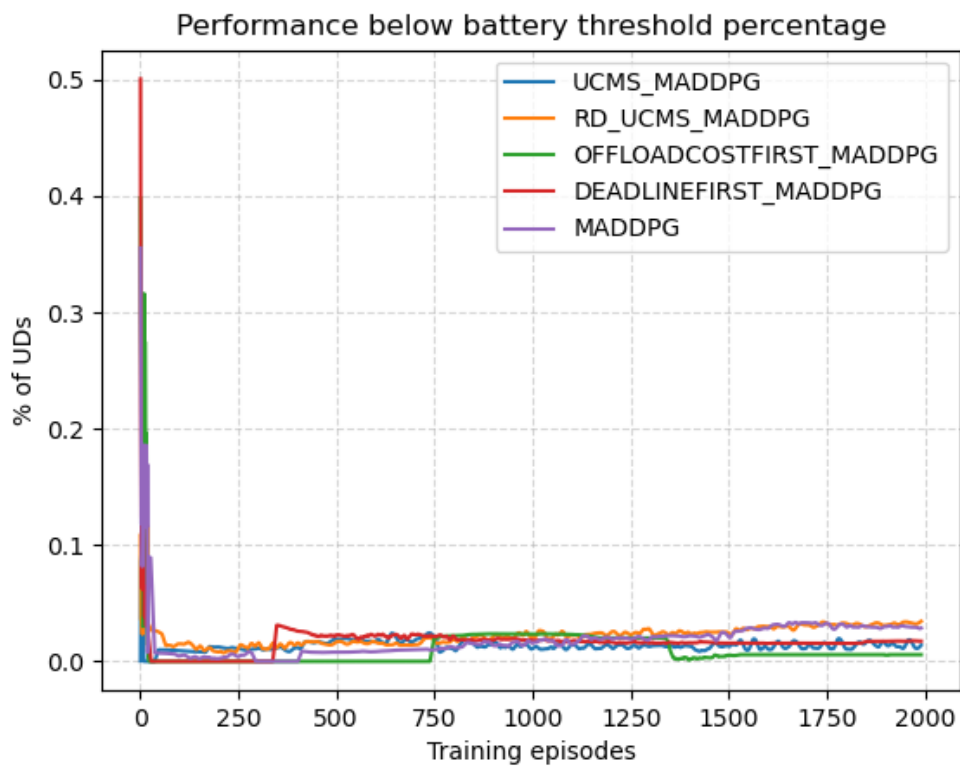


Fig.11 Percentage below the battery threshold for different algorithms in 100 time slots

6 Conclusion

This paper presents a user-centric DRL model splitting inference scheme to address the challenges in dynamic MEC environments, which involve multi-user, multi-server, and multi-angle resource constraints. The scheme aims to make efficient offloading decisions while minimizing task execution delay and energy consumption. Through decoupling the optimization problem, we introduce a user-server co-selection algorithm to tackle the selection issue between users and servers. Additionally, we leverage user-centric model splitting inference technology to design a UCMS_MADDPG-based offloading algorithm for task decision-making and response management. During the MDP transformation process, we split the action space into two distinct components to support hybrid decision-making, where the final offloading decision is derived by considering both continuous and discrete actions. Furthermore, a preferential sampling mechanism based on reward error trade-off is introduced to enhance the strategy's performance. Simulation results confirm the convergence of UCMS_MADDPG and show its superior performance in dynamic environments, confirming its effectiveness in optimizing both delay and energy consumption.

References

- [1] Matin, A., Islam, R., Wang, X., Huo, H., & Xu, G. (2023). AIoT for sustainable manufacturing: Overview, challenges, and opportunities. *Internet of Things*, 24, 100901.
- [2] Qian, L., Luo, Z., Du, Y., & Guo, L. (2009). Cloud computing: An overview. *Lecture Notes in Computer Science*, 5931, 626–631.
- [3] Mao, Y., You, C., Zhang, J., Huang, K., & Letaief, K. B. (2017). A survey on mobile edge computing: The communication perspective. *IEEE communications surveys & tutorials*, 19(4), 2322-2358.
- [4] Huang, L., Feng, X., Zhang, L., Qian, L., & Wu, Y. (2019). Multi-server multi-user multi-task computation offloading for mobile edge computing networks. *Sensors*, 19(6), 1446.
- [5] Li, B., Yang, R., Liu, L., Wang, J., Zhang, N., & Dong, M. (2024). Robust computation offloading and trajectory optimization for multi-UAV-assisted MEC: A multi-agent DRL approach. *IEEE Internet of Things Journal*, 11(3), 4775–4786.
- [6] Yan, M., Xiong, R., Wang, Y., & Li, C. (2023). Edge computing task offloading optimization for a UAV-assisted internet of vehicles via deep reinforcement learning. *IEEE Transactions on*

Vehicular Technology, 73(4), 5647–5658.

- [7] Mi, X., He, H., & Shen, H. (2024). A multi-agent RL algorithm for dynamic task offloading in D2D-MEC network with energy harvesting. *Sensors*, 24(9), 2779.
- [8] Wu, Y.-C., Dinh, T. Q., Fu, Y., Lin, C., & Quek, T. Q. (2021). A hybrid DQN and optimization approach for strategy and resource allocation in MEC networks. *IEEE Transactions on Wireless Communications*, 20(7), 4282-4295.
- [9] Hu, H., Wu, D., Zhou, F., Jin, S., & Hu, R. Q. (2021). Dynamic task offloading in MEC-enabled IoT networks: A hybrid DDPG-D3QN approach. *2021 IEEE Global Communications Conference (GLOBECOM)*, 1–6.
- [10] Dulac-Arnold, G., Evans, R., Hado van Hasselt, Sunehag, P., Lillicrap, T., Hunt, J., Mann, T., Weber, T., Degris, T., & Coppin, B. (2015). Deep reinforcement learning in large discrete action spaces. *ArXiv preprint arXiv: 1512.07679*.
- [11] Huang, C., Zhang, H., Wang, L., Luo, X., & Song, Y. (2022). Mixed deep reinforcement learning considering discrete-continuous hybrid action space for smart home energy management. *Journal of Modern Power Systems and Clean Energy*, 10(3), 743-754.
- [12] Hu, T., Luo, B., Yang, C., & Huang, T. (2023). MO-MIX: Multi-objective multi-agent cooperative decision-making with deep reinforcement learning. *IEEE Transactions on Pattern Analysis and Machine Intelligence*, 45(10), 12098–12112.
- [13] Yan, J., Bi, S., Zhang, Y. J., & Tao, M. (2020). Optimal task offloading and resource allocation in mobile-edge computing with inter-user task dependency. *IEEE Transactions on Wireless Communications*, 19(1), 235-250.
- [14] Zhang, J., Du, J., Shen Y., & Wang, J. (2020). Dynamic computation offloading with energy harvesting devices: A hybrid decision based deep reinforcement learning approach. *IEEE Internet of Things Journal*, 7(10), 9303–9317.
- [15] Tariq, M. N., Wang, J., Memon, S., Siraj, M., Altamimi, M., & Mirza, M. A. (2024). Towards energy-efficiency: Integrating DRL and ze-RIS for task offloading in UAV-MEC environments. *IEEE Access*, 12, 65530–65542.
- [16] Wu, H., Wolter, K., Jiao, P., Deng, Y., Zhao, Y., & Xu, M. (2021). EEDTO: An energy-efficient dynamic task offloading algorithm for blockchain-enabled IoT-edge-cloud orchestrated computing. *IEEE Internet of Things Journal*, 8(4), 2163-2176.
- [17] Yang, J., Yuan, Q., Chen, S., He, H., Jiang, X., & Tan, X. (2023). Cooperative task offloading for mobile edge computing based on multi-agent deep reinforcement learning. *IEEE Transactions on Network and Service Management*, 20(3), 3205-3219.
- [18] Chen, J., Xing, H., Xiao, Z., Xu, L., & Tao, T. (2021). A DRL agent for jointly optimizing

- computation offloading and resource allocation in MEC. *IEEE Internet of Things Journal*, 8(24), 17508–17524.
- [19] Nguyen, D., Ding, M., Pathirana, P., Seneviratne, A., Li, J., & Poor, V. (2021). Cooperative task offloading and block mining in blockchain-based edge computing with multi-agent deep reinforcement learning. *IEEE Transactions on Mobile Computing*, 22(4), 2021–2037.
- [20] Gong, B., & Jiang, X. (2023). Dependent task-offloading strategy based on deep reinforcement learning in mobile edge computing. *Wireless Communications and Mobile Computing*, 2023(1), 4665067.
- [21] Dong, J., Chen, L., Zheng, C., Pan, K., Guo, Q., Wu, S., & Wang, Z. (2024). A hierarchical optimization approach for industrial task offloading and resource allocation in edge computing systems. *Cluster Computing*, 27(5), 5981–5993.
- [22] Zhao, T., He, L., Huang, X., & Li, F. (2022). DRL-based secure video offloading in MEC-enabled IoT networks. *IEEE Internet of Things Journal*, 9(19), 18710-18724.
- [23] Du, R., Wang, J., & Gao, Y. (2024). Computing offloading and resource scheduling based on DDPG in ultra-dense edge computing networks. *The Journal of Supercomputing*, 80(8), 10275-10300.
- [24] Liu, Q., Zhang, H., Zhang, X., & Yuan, D. (2024). Joint service caching, communication and computing resource allocation in collaborative MEC systems: A DRL-based two-timescale approach. *IEEE Transactions on Wireless Communications*, 23(10), 15493–15506.
- [25] Lee, I. S. K., & Lau, H. Y. K. (2004). Adaptive state space partitioning for reinforcement learning. *Engineering Applications of Artificial Intelligence*, 17(6), 577–588.
- [26] Yuan, M., Zhang L., Yao, Y. H., Zhang, J. Y., Lou, P. H., & Li, X. Y. (2024). Resource-efficient model inference for AIoT: A survey. *Chinese Journal of Computers*(10), 2247-2273.
- [27] Xiong, J., Guo, P., Wang, Y., Meng, X., Zhang, J., Qian, L., & Yu, Z. (2023). Multi-agent deep reinforcement learning for task offloading in group distributed manufacturing systems. *Engineering Applications of Artificial Intelligence*, 118, 105710.